Optica Applicata, Vol. XLI, No. 3, 2011

Unconventional photonic gaps of a one dimensional photonic band gap structure

MUNAZZA ZULFIQAR ALI

Department of Physics, Punjab University, Quaid-i-Azam Campus, Lahore, Pakistan

We present a scheme to realize the zero–n gap and the zero–ϕ_{eff} gap in a one dimensional photonic band gap structure containing metamaterials. The electric permittivity and the magnetic permeability of the layers of the structure are represented by the Drude model and the resonant model. In a certain frequency range, the chosen structure behaves as a structure of alternate double negative and double positive layers to exhibit a zero–n gap. In another frequency range, it behaves as a structure of alternate permittivity negative and permeability negative layers to exhibit a zero–ϕ_{eff} gap. Some properties and benefits of having the zero–n and the zero–ϕ_{eff} gap in the same physical system are discussed.

Keywords: photonic band gap structures, metamaterials, zero–n gap, zero–ϕ_{eff} gap.

1. Introduction

Recently, the experimental realization [1–3] of single and double negative metamaterials has opened up a new research area. Metamaterials are such artificial periodic structures in which the dimensions of the periodically repeated elements are much smaller than the wavelength of the incident light so that the structure appears to be a homogenous medium for the working wavelength. The metamaterials in which both electric permittivity and magnetic permeability are negative are known as double negative (DNG) or left-handed (LH) materials and those in which only one of these quantities has a negative value are known as single negative materials (SNG). The SNG metamaterials having negative values of electric permittivity are known as ENG and those having negative value of magnetic permeability are known as MNG. The inclusion of DNG and SNG metamaterials in photonic band gap (PBG) structures has led to the emergence of new mechanisms to produce photonic gaps. These unconventional photonic gaps have certain advantages as compared to the conventional Bragg gaps. A zero–n gap has been found in a one dimensional PBG structure containing alternate DNG and DPS (double positive, *i.e.*, regular material) layers in the frequency range in which the average refractive index of the structure becomes zero [4, 5] whereas a zero–ϕ_{eff} gap emerges due to a mismatch in the local phase shifts of the two layers around the wave impedance matching frequency [6, 7].

The SNG or DNG metamaterials have been experimentally realized in the form of three-dimensional array of very long, thin continuous wires in which cuts are

periodically introduced and in the form of split ring resonators. The simplest theoretical models which describe the effective electric permittivity and magnetic permeability of these structures are the Drude model and the resonant model [8, 9] in which the values of the plasma frequency and the resonant frequency depend upon the structure parameters and it is possible to shift them to a desirable value by changing the structure parameters. These models are essentially dispersive so that these behaviors are limited in a certain frequency range and in other frequency ranges their permittivity and permeability have different signs. The PBG structures containing alternate DNG and DPS materials exhibit a zero–n gap in a certain frequency range and conventional Bragg gaps in other frequency ranges. The PBG structures containing alternate ENG and MNG layers exhibit a zero–ϕ_{eff} gap in a certain frequency range and conventional Bragg gaps in other frequency ranges. Here we theoretically suggest a PBG structure that can support both a zero–n gap and a zero–ϕ_{eff} gap in different frequency ranges. By suitably adjusting the values of the resonant frequency and the plasma frequencies in this structure, there exists a frequency range in which the structure behaves as having alternate left-handed and right-handed layers so that the average refractive index becomes zero in a certain frequency range to produce a zero–n gap. In the same structure there also exists a higher frequency range in which the system behaves as having alternate ENG and MNG layers to produce a zero–ϕ_{eff} gap. Although the zero–n gap and the zero–ϕ_{eff} gap result from different mechanisms, they share many properties, which are quite distinct as compared to those of Bragg gaps as shown in many recent studies. These gaps are relatively insensitive to scaling, disorder, incident angle and polarization of the incident light [10–17]. The appearance of the zero–n and zero–ϕ_{eff} gaps in the same physical system can be utilized in certain applications as discussed later.

2. Theoretical model and calculations

Here we study a one-dimensional PBG structure of two alternate layers A and B. The electric permittivity and the magnetic permeability of layer A are represented by the Drude model. The electric permittivity of layer B is represented by the resonant model and its magnetic permeability is assumed to have constant value equal to 1.

$$\varepsilon_A = 1 - \frac{\omega_{eA}^2}{\omega^2 + i\gamma_A\omega}, \qquad \mu_A = 1 - \frac{\omega_{mA}^2}{\omega^2 + i\gamma_A\omega} \tag{1}$$

$$\varepsilon_B = 1 - \frac{\omega_{eB}^2 - \omega_{0B}^2}{\omega^2 - \omega_{0B}^2 + i\gamma_B\omega}, \qquad \mu_B = 1 \tag{2}$$

where ω_{mA} and γ_A represent magnetic plasma frequency and the damping coefficient of the layer A, respectively. For the layer B, ω_{eB}, ω_{0B} and γ_B represent the electric

plasma frequency, the resonant frequency and the damping coefficient, respectively. We have initially considered the effect of losses in Fig. 2**b**. It is obvious that the inclusion of the damping term results in a reduced value of the transmission coefficient but the position of the gap is not affected. In the remaining part of the paper, losses are ignored, *i.e.*, $\gamma_A = \gamma_B = 0$, as done in most of the theoretical studies [10–16]. It is further assumed that internal dimensions of the metamaterials A and B are such that the assumptions of effective permittivity and effective permeability are valid throughout the frequency range under consideration. The tangential components of the electric and magnetic fields for a TE (transverse electric) wave across the *j*-th layer are related by the following transfer matrix:

$$m_j = \begin{bmatrix} \cos(k_j d_j) & -\dfrac{1}{q_j}\sin(k_j d_j) \\ q_j \sin(k_j d_j) & \cos(k_j d_j) \end{bmatrix} \tag{3}$$

where

$$k_j = \frac{\omega}{c}\sqrt{\mu_j}\,\sqrt{\varepsilon_j}\,\sqrt{1 - \frac{\sin^2\theta}{\mu_j\,\varepsilon_j}} \tag{4a}$$

$$q_j = \frac{\sqrt{\varepsilon_j}}{\sqrt{\mu_j}}\sqrt{1 - \frac{\sin^2\theta}{\mu_j\,\varepsilon_j}} \tag{4b}$$

The tangential components of the electric and magnetic fields at the incident side $x = 0$ and at the transmitted side $x = L$ are related by:

$$\begin{bmatrix} E_1 \\ H_1 \end{bmatrix}_{x=0} = M \begin{bmatrix} E_N \\ H_N \end{bmatrix}_{x=L} \tag{5}$$

where:

$$M = \prod_{j=1}^{N+1} m_j \tag{6}$$

where N is the total number of layers in the structure. The transmission coefficient T of the finite structure is calculated by applying the boundary conditions at the incident and the transmitted ends and is given by the following expression:

$$T = \frac{2q_0}{(q_0 M_{11} + q_0 M_{22}) - (q_0^2 M_{12} + M_{21})} \tag{7}$$

where $q_0 = [1 - \sin^2\theta/\varepsilon_0\mu_0]^{1/2} = \cos\theta$, as there is air, *i.e.*, $\varepsilon_0 = \mu_0 = 1$ (in cgs units) on the incident and the transmitted sides of the structure. M_{lm} is the element of the matrix M.

In our computational work, we have used dimensionless units, *i.e.*, frequency is given by $W = \omega d/c$ and the widths are given by $D_i = d_i/d$, $i = A, B$, where $d = d_A + d_B$ and c is the velocity of light. The advantage of using these dimensionless units is that the widths belonging to any length scale and the corresponding values of frequencies can fit these calculations, however since the double and single negative metamaterials have been realized in GHz frequency range, the realistic values that can be used for this scheme can be chosen as: $\omega_{eA} = 2\pi\times3.01$ GHz, $\omega_{mA} = \omega_{eB} = 2\pi\times4.77$ GHz, $\omega_{0B} = 2\pi\times2.34$ GHz, $d_A = 27$ mm, $d_B = 23$ mm.

The frequency dispersions of electric permittivities and magnetic permeabilities of the two layers are shown in Fig. 1. Here we consider two frequency ranges. For frequencies which lie below the resonant frequency of the layer B, the electric permittivity of layer B is positive, as its magnetic permittivity is chosen to be one, so for $\omega < \omega_{0B}$, the layer B behaves as DPS material. Here we have chosen the values of

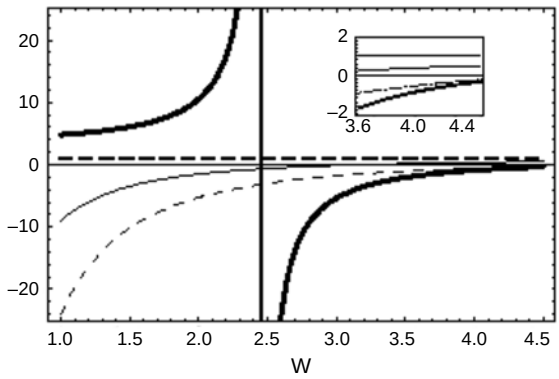

Fig. 1. The curves show the frequency dispersion of the electric permittivities and the magnetic permeabilities of the two layers. On the horizontal axis the frequency is in dimensionless units. The thin lines correspond to layer A and the thick lines correspond to layer B. The solid lines show the behavior of the electric permittivity and the dashed lines show the behavior of the magnetic permeability of the two layers. The inset shows the blown up version of that part of the plot in which the structure behaves as having alternate ENG and MNG layers.

the electric and magnetic plasma frequencies of layer A such that in this frequency range the electric permittivity and magnetic permeability of layer A are negative so that it behaves as DNG material. The structure is composed of alternate DPS and DNG layers in this frequency range. Initially we have considered the normally incident wave, *i.e.*, $\theta = 0°$. The average refractive index of the structure is defined by:

$$n_{\mathrm{av}} = n_A D_A + n_B D_B \tag{8}$$

where

$$n_A = \sqrt{\varepsilon_A}\,\sqrt{\mu_A} \tag{9a}$$

$$n_B = \sqrt{\varepsilon_B}\,\sqrt{\mu_B} \tag{9b}$$

This average refractive index is plotted in Fig. 2**a**. It becomes zero when the frequency is nearly 2 (in dimensionless units), so a zero–*n* gap appears around this frequency, as shown in Fig. 2**b**.

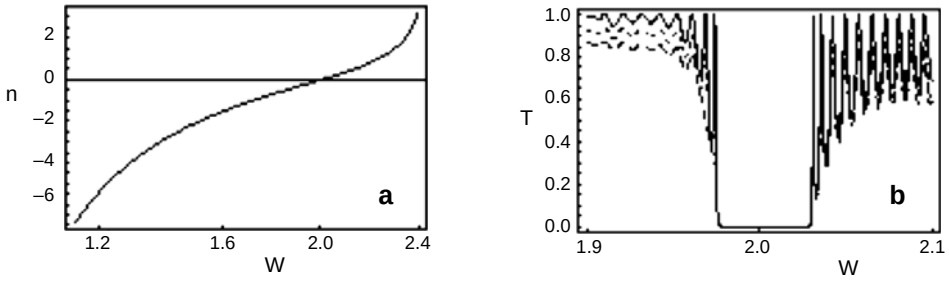

Fig. 2. The average refractive index of the structure becomes zero at a certain frequency (**a**) which gives rise to the formation of a zero-*n* gap, as shown in the transmission spectrum of the structure (**b**). The frequency on the horizontal axes is in dimensionless units and $N = 30$. The dashed, dotted and the solid lines correspond to $\gamma_A = \gamma_B = 2\pi\times0.01$, $2\pi\times0.1$ and 0 GHz.

Next we consider the frequency range $\omega_{eA} < \omega < \omega_{mA}$, in which layer A behaves as MNG layer since its electric permittivity becomes positive but the magnetic permeability remains negative. As $\omega_{0B} < \omega_{mA}$, layer B behaves as ENG layer since its permittivity has negative value in this frequency range. So the structure behaves as having alternate MNG and ENG layers in this frequency range. The impedance of the *i*-th layer is defined by:

$$z_i = \frac{\sqrt{|\mu_i|}}{\sqrt{|\varepsilon_i|}} \qquad i = A, B \tag{10}$$

This has been plotted in Fig. 3**a**. The impedances of the two layers match at a frequency which is nearly equal to 4.1, as there is a mismatch in the effective phase shift of the two layers, *i.e.*, $|k_A| d_A \neq |k_B| d_B$ at this wave impedance matching frequency, so a gap is opened up around this frequency, as shown in Fig. 3**b**. This gap is known as the zero–ϕ_{eff} gap [6, 7].

The zero–*n* gap is surrounded by propagating modes whereas the zero–ϕ_{eff} gap is surrounded by tunneling modes, but the remarkable thing is that both gaps emerge due to some averaging effect produced by the structure in contrast to the conventional

gaps which result due to Bragg reflections. It has already been discussed in great detail in many investigations [4–7, 10–17] that both the zero–n gap and the zero–ϕ_{eff} gap are relatively insensitive to the scaling, disorder, incident angle and polarization of the incident light when compared to Bragg gaps. Moreover, it has been shown that the defect modes which reside within the zero–n and the zero–ϕ_{eff} gaps are found to be insensitive to scaling, disorder, incident angle and polarization of the light when compared to those which reside inside Bragg gaps [10, 14]. There is no point in re-investigating all these properties here, however to show that these properties are exhibited in this scheme as well, we have considered the case of the angular dependence of these gaps for linear as well as nonlinear wave propagation. Figure 4 shows that the position of the zero–n gap on the frequency axis is very slightly affected when the angle of incidence varies appreciably, *i.e.*, from 10° to 30°. The same effect can be shown for the zero–ϕ_{eff} gap, however we have shown the insensitiveness of the zero–ϕ_{eff} gap to the incident angle by considering nonlinear

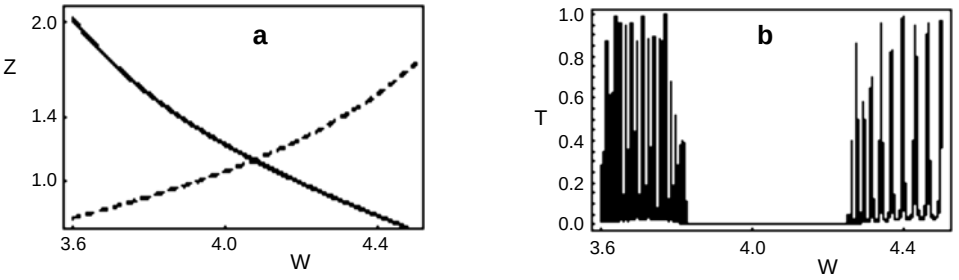

Fig. 3. The impedance of the two layers – solid line corresponds to layer A and dotted line corresponds to layer B (**a**). At a certain frequency, the impedances of the two layers match which gives rise to the opening up of the zero–ϕ_{eff} gap as the effective phase shift in the two layers is not same at this wave impedance matching frequency (**b**). The frequency on the horizontal axis is in dimensionless units and $N = 30$.

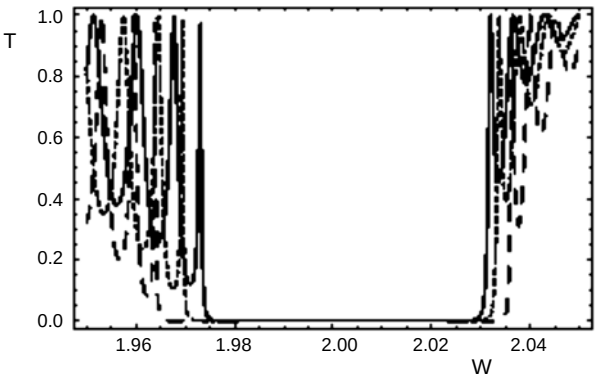

Fig. 4. Angular dependence of the zero–n gap. The continuous, dotted and dashed curves correspond to the incident angles $\theta = 10°, 20°, 30°$, respectively. All other parameters are same as in Fig. 2.

wave propagation. The electric permittivity of layer A is now taken to have Kerr type nonlinearity, *i.e.*, it can be represented by:

$$\varepsilon_A = 1 - \frac{\omega_{eA}^2}{\omega^2} + \lambda \left| E_A \right|^2 \tag{11}$$

As the layers are assumed to be thin, the transmission coefficient for the nonlinear wave propagation can be calculated by using the nonlinear characteristic matrix approach [18]. The electric field in the nonlinear layer can be written as:

$$E_A(x) = E_A^+ \exp(ik_A^+ x) + E_A^- \exp(ik_A^- x) \tag{12}$$

where the values of k_A^+ and k_A^- are given as:

$$k_A^+ = \sqrt{\frac{\omega^2}{c^2}\mu_A \varepsilon_{0A} + \lambda \frac{\omega^2}{c^2}\mu_A \left(\left| E_A^+ \right|^2 + 2 \left| E_A^- \right|^2 \right)} \tag{13a}$$

$$k_A^- = \sqrt{\frac{\omega^2}{c^2}\mu_A \varepsilon_{0A} + \lambda \frac{\omega^2}{c^2}\mu_A \left(\left| E_A^- \right|^2 + 2 \left| E_A^+ \right|^2 \right)} \tag{13b}$$

The values of E_A^- and E_A^+ are determined as functions of k_A^+ and k_A^- by applying the boundary conditions at the interface of the nonlinear layer and are substituted in the above equations to get two coupled nonlinear equations in k_A^+ and k_A^-. These coupled nonlinear equations are solved numerically to determine the values of k_A^+ and k_A^-. The electric and magnetic field components across the nonlinear layer are related by the following transfer matrix

$$m_A = \begin{bmatrix} X_1 & X_2 \\ X_3 & X_4 \end{bmatrix} \tag{14}$$

where

$$X_1 = \frac{k_A^-}{k_A^- + k_A^+} \exp(ik_A^+ d_A) + \frac{k_A^+}{k_A^- + k_A^+} \exp(-ik_A^- d_A) \tag{15a}$$

$$X_2 = \frac{i\mu_A}{k_A^- + k_A^+} \left[\exp(ik_A^+ d_A) + \exp(-ik_A^- d_A) \right] \tag{15b}$$

$$X_3 = \frac{ik_A^+k_A^-}{\mu_A(k_A^- + k_A^+)}\left[\exp(ik_A^+d_A) + \exp(-ik_A^-d_A)\right] \tag{15c}$$

$$X_4 = \frac{k_A^+}{k_A^- + k_A^+}\exp(ik_A^+d_A) + \frac{k_A^-}{k_A^- + k_A^+}\exp(-ik_A^-d_A) \tag{15d}$$

So, the transmitted electric field can be determined by working layer as described above and the transmission coefficient is calculated in the usual manner.

Figure 5 shows the phenomenon of optical bistability for a frequency which lies inside the zero–ϕ_{eff} near its low frequency edge. The vertical axis shows the transmission coefficient T whereas the dimensionless control parameter $I = \lambda|E_{\text{in}}|^2$, which

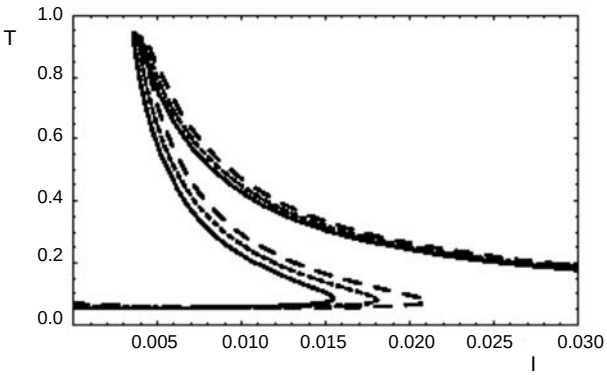

Fig. 5. Angular dependence of the bistability curve at $W = 3.7$ inside the zero–ϕ_{eff} gap. The continuous, dotted and dashed curves correspond to the incident angles $\theta = 10°$, 20°, 30°, respectively. The sign of Kerr coefficient is negative; all other parameters are same as in Fig. 3.

measures the incident intensity, is plotted on the horizontal axis. When the angle of incidence varies from 10° to 30°, the characteristics of the bistability curve are affected very slightly, whereas in the case of Bragg gap these characteristics are affected drastically, as discussed in detail in Ref. [16].

3. Results and discussion

The properties associated with the zero–n and zero–ϕ_{eff} gap are important for application purposes. The devices based on such gaps can be more compact, operate for wider angular incidences and can be relatively insensitive to the polarization of light. The presence of these two gaps in the same physical system can be more useful for application purposes as compared to a situation where one of them is present and the other gaps are conventional Bragg gaps. One way in which the presence of these two gaps can be beneficial is to use the same structure to work in two different frequency ranges to realize the useful properties of insensitivity to the incident angle

and the polarization of light. The availability of a zero–n gap and a zero–ϕ_{eff} gap in the same physical system can lead to some improvements in those applications in which dual modes in different frequency ranges are required, *i.e.*, dual channel filters for a wider angle filtering process and dual optical switches can also be designed based on the structure presented here. Recently, a giant enhancement of second harmonic generation has been suggested [19] by using a dual localization in the same defect where the frequency of the fundamental wave (FW) lies in one Bragg gap and that of the second harmonic (SH) lies in the higher Bragg gap. An improvement to this model was suggested [20] by using a 1D PBG structure containing alternate DNG and DPS layers because such a structure can possess a zero–n gap and many Bragg gaps. So, by suitably adjusting the parameters it was shown that dual localization inside the single defect can take place where FW resides inside zero–n gap and the SH resides inside a Bragg gap. The structure which we have suggested can possess a zero–n gap and a zero–ϕ_{eff} gap in different frequency ranges. So, by suitably adjusting the parameters, a single defect can produce dual localized modes, one belonging to the zero–n gap and the other lying inside the zero–ϕ_{eff} gap. Such a structure will have certain advantages due to the special characteristics associated with the zero–n and zero–ϕ_{eff} gaps. However, we want to mention here that the formation of dual defect modes in a disordered system is very complicated and requires careful consideration of the structure parameters which may fall out of scope of the present study but may lead to some further investigations.

In summary, the appearance of a zero–n gap and a zero–ϕ_{eff} gap is shown theoretically in a PBG structure containing two alternate metamaterials. These two gaps have certain advantages over Bragg gaps, *e.g.*, these are found to be insensitive to scaling, disorder, incident angle and polarization. The possibility of utilizing the presence of these two gaps in the same physical system for the improvement of certain applications is also discussed.

References

[1] SMITH D.R., KROLL N., *Negative refractive index in left-handed materials*, Physical Review Letters **85**(14), 2000, pp. 2933–2936.

[2] SHELBY R.A., SMITH D.R., SCHULTZ S., *Experimental verification of a negative index of refraction*, Science **292**(5514), 2001, pp. 77–79.

[3] SHELBY R.A., SMITH D.R., NEMAT-NASSER S.C., SCHULTZ S., *Microwave transmission through a two--dimensional, isotropic, left-handed metamaterial*, Applied Physics Letters **78**(4), 2001, pp. 489–491.

[4] ZHAROV A.A., SHADRIVOV I.V., KIVSHAR Y.S., *Nonlinear properties of left-handed metamaterials*, Physical Review Letters **91**(3), 2003, p. 037401.

[5] FEISE M.W., SHADRIVOV I.V., KIVSHAR Y.S., *Tunable transmission and bistability in left-handed band-gap structures*, Applied Physics Letters **85**(9), 2004, pp. 1451–1453.

[6] HAITAO JIANG, HONG CHEN, HONGQIANG LI, YEWEN ZHANG, JIAN ZI, SHIYAO ZHU, *Properties of one--dimensional photonic crystals containing single-negative materials*, Physical Review E **69**(6), 2004, p. 066607.

[7] LI-GANG WANG, HONG CHEN, SHI-YAO ZHU, *Omnidirectional gap and defect mode of one-dimensional photonic crystals with single-negative materials*, Physical Review B **70**(24), 2004, p. 245102.

[8] PENDRY J.B., HOLDEN A.J., STEWART W.J., YOUNGS I., *Extremely low frequency plasmons in metallic mesostructures*, Physical Review Letters **76**(25) 1996, pp. 4773–4776.
[9] PENDRY J.B., HOLDEN A.J., ROBBINS D.J., STEWART W.J., *Magnetism from conductors and enhanced nonlinear phenomena*, IEEE Transactions on Microwave Theory and Techniques **47**(11), 1999, pp. 2075–2084.
[10] HAITAO JIANG, HONG CHEN, HONGQIANG LI, YEWEN ZHANG, SHIYAO ZHU, *Omnidirectional gap and defect mode of one-dimensional photonic crystals containing negative-index materials*, Applied Physics Letters **83**(26), 2003, pp. 5386–5388.
[11] KUN-YUAN XU, XIGUANG ZHENG, WEI-LONG SHE, *Properties of defect modes in one-dimensional photonic crystals containing a defect layer with a negative refractive index*, Applied Physics Letters **85**(25), 2004, pp. 6089–6091.
[12] WOODLEY J.F., MOJAHEDI M., *Negative group velocity and group delay in left-handed media*, Physical Review E **70**(4), 2004, p. 046603.
[13] JIANG HAI-TAO, CHEN HONG, LI HONG-QIANG, ZHANG YE-WEN, *Omnidirectional gaps of one-dimensional photonic crystals containing single-negative materials*, Chinese Physics Letters **22**(4), 2005, pp. 884–886.
[14] HAITAO JIANG, HONG CHEN, HONGQIANG LI, YEWEN ZHANG, SHIYAO ZHU, *Compact high-Q filters based on one-dimensional photonic crystals containing single-negative materials*, Journal of Applied Physics **98**(1), 2005, p. 013101.
[15] WANG S.M., TANG C.J., PAN T., GAO L., *Bistability and gap soliton in one-dimensional photonic crystal containing single-negative materials*, Physics Letters A **348**(3–6), 2006, pp. 424–431.
[16] WANG S.M., GAO L., *Nonlinear responses of the periodic structure composed of single negative materials*, Optics Communications **267**(1), 2006, pp. 197–204.
[17] CHEN Y.H., DONG J.W., WANG H.Z., *Twin defect modes in one-dimensional photonic crystals with a single-negative material defect*, Applied Physics Letters **89**(14), 2006, p. 141101.
[18] BILBAULT J.M., REMOISSENET M., *Gap solitons in nonlinear electrical superlattices*, Journal of Applied Physics **70**(8), 1991, pp. 4544–4550.
[19] JING CHEN, FANG-FANG REN, RUI LI, NIAN-HAI SHEN, YA-XIAN FAN, JIANPING DING, HUI-TIAN WANG, *Dual localizations for second-harmonic generations using left-handed materials*, Applied Physics Letters **87**(25), 2005, p. 251104.
[20] FANG-FANG REN, RUI LI, CHEN CHENG, HUI-TIAN WANG, JIANRONG QIU, JINHAI SI, KAZUYUKI HIRAO, *Giant enhancement of second harmonic generation in a finite photonic crystal with a single defect and dual-localized modes*, Physical Review B **70**(24), 2004, p. 245109.

Received September 21, 2010
in revised form January 25, 2011